Soil Biology and Biochemistry 156 (2021) 108195

Contents lists available at ScienceDirect

Soil Biology and Biochemistry

journal homepage: http://www.elsevier.com/locate/soilbio

Nitrogen availability modulates the impacts of plant invasion on the chemical composition of soil organic matter

Ziliang Zhang *, Vidya Suseela

Department of Plant & Environmental Sciences, Clemson University, Clemson, SC, USA

ARTICLE INFO

Keywords:
Soil organic C
Plant invasion
Fertilizer application
Polygonum cuspidatum
Plant-derived C
Microbial-derived C

ABSTRACT

Plant invasion can dramatically impact soil carbon (C) cycling and sequestration while, other global change factors, such as nitrogen (N) deposition, are predicted to promote plant invasion. However, questions remain as to whether the chemical composition of soil organic C (SOC) may alter with plant invasion and how N availability modulates the invasion effects on SOC. In this study, we conducted a 10-year mesocosm experiment simulating the invasion of Japanese knotweed (*Polygonum cuspidatum*) into a fallow soil, coupled with a simultaneous mineral fertilizer application scheme for the invasive plants. We investigated the invasion effects on the chemical composition of various SOC components at the molecular level, and examined how these effects responded to changes in soil N availability. Compared with the noninvaded soils, the knotweed-invaded soils exhibited a 17% increase in the microbial-derived C, mainly through the accumulation of fungal residue in the form of amino sugars. Despite receiving leaf litter which was abundant in polyphenolic compounds (40% and 3-times higher in lignin and tannins per unit biomass, respectively), the knotweed-invaded soils did not differ in the concentration of plant lipids and lignin monomers compared to the noninvaded soils inhabited by grasses. However, the concentrations of phytosterol in the knotweed-invaded soils were 1.5-fold as that in the non-invaded soils. Fertilizer application significantly increased the retention of plant-derived compounds in the knotweed-invaded soils, but also induced 45% greater degradation of lignin. Moreover, under fertilizer application, the knotweed-invaded soils accumulated 46% more microbial-derived C, primarily due to the altered microbial biomass and community composition. Collectively, our findings suggest that plant invasion has the potential to influence SOC chemical composition through changes in plant-derived and microbial-derived C. Furthermore, N deposition could reinforce the invasion effects on the molecular composition and accrual of SOC. Our results also highlight the need to understand the impacts of biological invasion in the context of other global change drivers that both affect invasion and modulate their effects.

1. Introduction

Biological invasion represents one of the most significant elements of global change (Bradley et al., 2010; Simberloff et al., 2013), as invasion of exotic species not only poses major threats to the native biodiversity, but also potentially impacts ecosystem stability and functions such as carbon (C) storage and cycling (Liao et al., 2008; Craig et al., 2015). As soils store the largest organic C pool in terrestrial ecosystems (Schmidt et al., 2011; Lehmann and Kleber, 2015), widespread changes in soil C stock and stability due to plant invasion could have profound implications for atmospheric CO_2 concentrations and the global C cycle. Previous studies have reported contrasting influences of invasive plants on soil organic C (SOC) accrual (Jackson et al., 2002; Vila et al., 2011; Yang et al., 2016). Although meta-analyses regarding the effects of plant invasion on soil C cycling induced an overall increase in soil C sequestration due to enhanced above- and below-ground biomass inputs and/or decreased litter decomposition (Liao et al., 2008; Vila et al., 2011), some studies have reported loss or no significant changes in soil C stock following plant invasion (Hughes et al., 2006; Strickland et al., 2010; Shang, 2013). These discrepancies may be attributed to the complex plant-soil feedbacks (Schmidt et al., 2011). Specifically, the response of SOC to plant invasion could be influenced by multiple factors, including plant functional traits (i.e., foliar photosynthetic traits, litter chemical traits, and root physiological and morphological traits), soil nutrient conditions, and microbial community (Dijkstra et al., 2004; Tamura and Tharayil, 2014; McTee et al., 2017). For example, exotic

* Corresponding author. Biosystems Research Complex (BRC), 105 Collings Street, Clemson University, Clemson, SC, 29634-0310, USA.
E-mail address: zilianz@clemson.edu (Z. Zhang).

https://doi.org/10.1016/j.soilbio.2021.108195
Received 29 September 2020; Received in revised form 19 February 2021; Accepted 28 February 2021
Available online 4 March 2021

species having a higher specific leaf area and a higher net photosynthetic rate may have the capacity to assimilate more C and incorporate it into native soil through litter inputs or root exudation (Liao et al., 2008). However, higher labile C inputs from invasive species with high-quality litter have also been found to cause a 'priming effect' by stimulating the catabolic activity of microbes, leading to reduced SOC stocks (Tamura and Tharayil, 2014). In addition, the counteracting effects of plant invasion on various C pools (e.g., different physical fractions) make the detection of changes in SOC dynamics difficult and uncertain (Tamura et al., 2017; Craig et al., 2019). Therefore, there remains a knowledge gap of how plant invasion impacts soil C stock and controls the stability and turnover of SOC, which hampers efforts to predict long-term soil C cycling in the context of global changes.

It is increasingly recognized that soil organic matter, which provides the basis for C sequestration, comprises a multitude of analytically identifiable structures rather than the traditionally defined "humic substances" with chemical structures unknown (Lehmann et al., 2008; Liang et al., 2019). SOC is composed of a myriad of biomolecules with different residence times, ranging from several minutes to thousands of years (Angst et al., 2017; Sokol and Bradford, 2019). These chemically distinct molecules could be distributed in different C pools. More specifically, the labile C pool constitutes easily degradable compounds such as sugars and proteins, and the recalcitrant C pool consists of macromolecular lipids and compounds containing aromatic ring structures which are more resistant to microbial decomposition (Cotrufo et al., 2015; Tamura et al., 2017). Long-term C sequestration requires the formation and accumulation of recalcitrant SOC which constitutes the largest fraction of soil C (Feng et al., 2010; Schmidt et al., 2011). Conventionally, plant-derived C compounds such as lignin have commonly been regarded as a major contributor to stabilized SOC pools because of their recalcitrance and preferential accumulation in the decomposing litter (Feng et al., 2010; Thevenot et al., 2010). However, there is growing consensus that products of microbial transformation of plant materials are likely to have a more important contribution to stable SOC formation than plant-derived compounds (Liang and Balser, 2012; Ma et al., 2018). This emerging mechanism of soil C accrual through the "microbial C pump" involves *in vivo* processing of plant-derived compounds, accumulation of microbial biomass and residue, deposition of microbial-derived molecules (e.g., degradative lignin products and amino sugars), and the subsequent formation of mineral-stabilized SOC (Liang et al., 2017; Minerovic et al., 2018). Therefore, elucidating the contributions of plant-derived and microbial-derived C components to the accrual of SOC pools is instrumental in understanding soil C dynamics under global changes. However, most current studies on SOC stabilization mainly focused on C storage in bulk soil or soil physical fractions (Lichter et al., 2008; Vestergard et al., 2016; Craig et al., 2019), with relatively little information about the dynamics of diversified chemical compositions of SOC and their response to changing environments (Feng et al., 2010; Tamura and Tharayil, 2014). The sole consideration of C stock in bulk soil with chemical structures largely uncharacterized at the molecular level does not allow insights into mechanisms accounting for the stabilization or loss of specific SOC constituents; it also does not permit the detection and prediction of subtle changes in soil C dynamics (Belay-Tedla et al., 2009). Although previous research has explored the effect of plant invasion on soil C cycling (Liao et al., 2008; Craig et al., 2015; McTee et al., 2017), questions remain as to whether the chemical components of SOC will be influenced by the invasion of exotic plant species and further modulated by other global change factors such as nitrogen (N) deposition.

Nutrient (mainly N) availability has been considered as a primary limiting factor for fast-growing plants, especially invasive species (Funk and Vitousek, 2007; Craig et al., 2015). Increased N deposition, largely caused by fertilizer application and fossil fuel combustion, is dramatically enhancing the supply of available N (Vitousek et al., 1997; Galloway et al., 2008). Such changes in N availability will significantly alter plant community by affecting the competition between exotic and native plants (Dijkstra et al., 2004). It has been hypothesized that N deposition in N-limited ecosystems will facilitate invasion because vigorous invasive plants are usually more aggressive with respect to resource competition and are more effective at resource acquisition compared to native plants (Bradley et al., 2010; van Kleunen et al., 2010). Accumulated evidence shows that elevated N deposition will increase the biomass of invasive species, and simultaneously induce a decrease of native species biomass (Brooks, 2003; Blumenthal et al., 2008), suggesting that plant invasion will be further promoted by the continuous increase in N deposition during the coming decades (Bradley et al., 2010). Although the roles of N availability in affecting the persistence and success of invasive species have been well recognized (Vitousek et al., 1997; Funk and Vitousek, 2007), it remains largely unexplored how N availability modulates the effects of plant invasion on the accrual, composition, and stability of SOC.

To date, a majority of studies in invasion ecology have been performed in the invaded ecosystems by pairwise comparing soils under native vegetation with those invaded by exotic species (Tamura and Tharayil, 2014; Stefanowicz et al., 2017; Craig et al., 2019). This research approach provided authentic information in situ, but also could result in some caveats such as the possibility of confounding effects of site history and invasion (Stefanowicz et al., 2018). Therefore, considering the potential limitations of field studies, it is instrumental to complement field studies with manipulated experiments by growing invasive plants in standardized soil conditions.

In this study, we selected Japanese knotweed (*Polygonum cuspidatum*) as a model species to investigate the effect of plant invasion on the chemical composition of SOC pools at the molecular level. We also set up a mineral fertilizer application system for the invasive plants to further determine how N availability modulates the effects of plant invasion on the composition of SOC. *P. cuspidatum* is now a widespread and problematic invader, which like most polyphenol-rich, yet fast-growing invasive species, can have undue impacts on the dynamics of SOC chemistry via an input of disproportionate quantities of chemically distinct above- and below-ground litter in ecosystems they invade (Tamura et al., 2017; Zhang et al., 2020). Moreover, *P. cuspidatum* could alter the spatial and temporal variability of mineral nutrient availability (Tharayil et al., 2013), making it an appropriate species to couple the effect of plant invasion with altered N availability. We measured the major soil organic matter biomarkers including extractable and hydrolyzable lipids, lignin-derived phenol, and amino sugars to assess the inputs and sequestration of source-specific compounds (i.e., plant-derived and microbial-derived C components). We also quantified the soil microbial biomass and community composition to elucidate potential mechanisms driving the variation of SOC compositions. We hypothesized that, (i) compared to the noninvaded soils, the knotweed-invaded soils would be characterized by a higher proportion of plant-derived C components but a lower proportion of microbial-derived C components, given that *P. cuspidatum* exhibits a low-quality litter input which is abundant in recalcitrant secondary compounds such as lignin and polyphenols (Tharayil et al., 2013; Suseela et al., 2016); (ii) fertilizer application would lead to further enrichment of plant-derived recalcitrant structures in the invaded soils through stimulating above-ground inputs, but simultaneously inhibiting the decomposition of lignified components due to altered microbial community.

2. Materials and methods

2.1. Experimental setup and sampling

P. cuspidatum is a perennial, herbaceous plant species that was introduced to Europe and North America from East Asia as an ornamental plant, a source of fodder, or a plant to stabilize soil in coastal areas (Barney et al., 2006; Suseela et al., 2016). *P. cuspidatum* is a

noxious weed, which has been listed as one of the world's worst invasive species by the World Conservation Union (Lowe et al., 2000), and is widely spread in 45 states in the United States and nearly all province in Canada (Zhang et al., 2020). To experimentally assess the effects of *P. cuspidatum* encroachment on SOC chemistry, we performed a soil conditioning experiment with *P. cuspidatum* planted in a standardized soil.

Soils for the experiment were collected in 2009 from the Musser Fruit Research Farm of the Clemson University in Seneca, South Carolina, USA (34° 36′N, 82° 52′W, and 221 m a.s.l.). The mean annual temperature is 16.1 °C with a maximum monthly mean air temperature of 26 °C in July and a minimum of 5.9 °C in January. Annual precipitation is 1325 mm. The soil is classified as Cambic Umbrisols according to the IUSS Working Group (2007). The soil was taken randomly to a depth of approximately 30 cm. Collected soils were homogenized and then filled in the experimental pots (65 cm high × 60 cm radius). The rhizomes of *P. cuspidatum* were gathered in 2008 from Greenville, South Carolina (34° 50′N, 82° 23′W), and were planted in March 2009 directly in the experimental pots. The following plant treatments were established in each soil (1) bare soil (hereafter noninvaded; 4 replicates), (2) *P. cuspidatum* (hereafter invaded; 8 replicates), and (3) *P. cuspidatum* with fertilizer application (hereafter invaded + fertilized; 8 replicates), giving a total of 20 pots. One replicate of the invaded + fertilized treatment was incorporated into the noninvaded treatment due to the lack of establishment of *P. cuspidatum*. One year after treatments, the noninvaded pots have been inhabited by native grass and forb species dominated by *Cynodon dactylon* and *Plantago asiatica*, due to the local seed bank and seed rain. The pots were randomly arranged (Fig. S1) and kept under natural atmospheric and light conditions in the Musser Fruit Research Farm for ten growing seasons from 2009 to the present. The plants were watered weekly in spring and summer with an automatic irrigation system when precipitation was insufficient. When the above-ground tissue of *P. cuspidatum* was developed one year after setting up the rhizomes, 7 pots designed for fertilizer application were treated with Miracle-Gro® Water Soluble All-Purpose Plant Food (Scotts Miracle-Gro Company, USA), a commonly used inorganic fertilizer for plant growth (Glenn et al., 2012; Shinohara and Leskovar, 2014). The main components of this fertilizer are N (24%), phosphorus (P; 8%), and potassium (16%) derived from urea, potassium phosphate, and potassium chloride, respectively. Fertilizer was applied bi-annually, in May and October. The annual doses were 150 kg N ha^{-1}, 75 kg P_2O_5 ha^{-1}, and 75 kg K_2O ha^{-1} based on previous long-term fertilizer application experiments (Wei et al., 2008; Ding et al., 2016).

In May 2019, after carefully removing the surface organic layer, soils from each pot were collected from the mineral layer (0–15 cm) using a 5-cm diameter soil corer. Samples from three points in each pot were thoroughly mixed to obtain one composite sample and were immediately kept on ice and transported to the laboratory. Each composite sample was passed through a 2-mm sieve, and any non-soil material and rocks were manually picked out from the sieved soil. The sieved soil samples were divided into three subsamples, with one subsample analyzed within 48 h after collection to determine the soil N availability, with a second subsample air-dried to determine the content and chemical composition of SOC, and with a third subsample stored at −20 °C for the analysis of microbial community composition.

Above-ground litter from each pot was harvested at the end of the growing season (September 2019) to calculate the accumulated litter inputs by randomly selecting a 0.0225 m^{-2} quadrat. Litter samples were taken to the laboratory and oven-dried at 60 °C for 48 h, weighed, and then ground into a fine powder before further analysis.

2.2. Chemical analysis

2.2.1. Chemical composition of plant litter

Chemical compositions (plant lipids and lignin monomers) of the above-ground plant litter were characterized following the sequential chemical extractions (solvent extraction, base hydrolysis, and copper (II) oxide (CuO) oxidation) using biomarker analysis described in detail in section *2.2.3* (Characterization of SOC chemical composition by biomarker analysis). Condensed tannins in litter samples were quantified using the acid-butanol assay modified from Tharayil et al. (2011) using the commercially available proanthocyanidin as a standard. Briefly, 50 mg litter sample was weighed into a 2 ml glass vial, extracted with 1 ml of HCl-n-butanol (5: 95) at 95 °C for 1.5 h. After cooling at room temperature, the concentration of condensed tannin in the clear supernatant was quantified spectrophotometrically at 550 nm on a spectrophotometer (V-550; PP JASCO Inc., Japan).

2.2.2. Physicochemical characteristics of bulk soil

The SOC and total N contents in all samples were measured using an elemental analyzer (Carlo Erba NA 1500 Elemental Analyzer; Thermo Scientific, Lakewood, NJ, USA). The concentration of soil dissolved inorganic N (DIN) (the sum of NH_4^+–N and NO_3^-–N) was determined after being extracted with KCl solution. Briefly, 7 g of fresh soil from each sample was extracted with 35 ml of 2 M KCl extractant for 1 h on an end-over-end rotisserie shaker, and then filtered through a Whatman #1 filter. The filtered supernatant was immediately frozen at −20 °C until concentration analysis. The soil DIN concentration was measured colorimetrically on a flow segmented analyzer (Astoria-2, Astoria-Pacific Solution, Clackamas, Oregon). The total dissolved N (TDN) in the same KCl extract was measured on a C/N analyzer (TOC-Vcsh/ASI-V; Shimadzu Scientific, Kyoto, Japan). The concentration of dissolved organic N (DON) was calculated as follows: DON = TDN – DIN.

2.2.3. Characterization of the chemical composition of SOC by biomarker analysis

Lipids and lignin monomers: Sequential chemical extractions such as solvent extraction, base hydrolysis, and CuO oxidation were conducted to isolate solvent-extractable free lipids, hydrolyzable bound lipids (including phytosterol), and lignin-derived phenols, respectively (Otto and Simpson, 2007; Tamura and Tharayil, 2014; Tamura et al., 2017). Briefly, air-dried samples (1 g soil or 100 mg plant material) were sequentially extracted with 5 ml of methanol, dichloromethane: methanol (1:1; v/v), and dichloromethane in glass tubes. The three sequential extracts were combined, and 15 ml of deionized water was added to induce phase separation. The bottom layer of dichloromethane was collected and stored at −20 °C until analysis (Tamura and Tharayil, 2014). The air-dried residue from the above solvent extraction was incubated at 95 °C for 3 h with 5 ml of 1 N methanolic sodium hydroxide (NaOH) to extract hydrolyzable lipids (Tamura et al., 2017). After cooling to room temperature, the supernatant was transferred to a new glass tube. The residue was further extracted with 5 ml of dichloromethane: methanol (1:1; v/v). The two sequential extracts were combined and spiked with 62.5 μl of heneicosanoic methyl ester ($C_{21:0}$) (100 μg/ml in methanol) as an internal standard. The extracts were acidified to pH < 2 using 1.5 ml of 6 M HCl. Hydrolysable or bound lipids were recovered by liquid–liquid extraction with 15 ml of deionized water. The bottom layer of dichloromethane was collected and stored at −20 °C until analysis.

Following base hydrolysis extraction, the residue was further subjected to CuO oxidation to isolate lignin-derived phenols: the air-dried residue was mixed with 1 g CuO, 150 mg ammonium iron (II) sulfate hexahydrate [$Fe(NH_4)_2(SO_4)_2 \cdot 6H_2O$], and 15 ml of NaOH solution (2 M; sparged with argon) in teflon-lined acid digestion vessels. All vessels were flushed with argon in the headspace for 5 min and then incubated at 155 °C for 160 min. After cooling, the lignin oxidation products were spiked with 100 μl of the internal standard (transcinnamic acid and ethylvanillin; 200 μg/ml in methanol) and acidified to pH < 2 using 3 ml of 18 N H_2SO_4. After centrifugation, 2 ml of pre-cooled ethyl acetate was added to the clear supernatant to induce phase separation. The upper layer of ethyl acetate was collected and stored at −20 °C until analysis. Lignin-derived phenols included vanillyls (V; vanillin, acetovanillone,

and vanillic acid), syringyls (S; syringaldehyde, acetosyringone, and syringic acid), and cinnamyls (C; p-coumaric acid and ferulic acid). Besides the lignin monomer contents, we also calculated the acid/aldehyde ratios of vanillyls [$(Ad/Al)_v$] and syringyls [$(Ad/Al)_s$], which typically increase with increasing lignin degradation (Otto and Simpson, 2007; Feng et al., 2010; Wang et al., 2015).

Aliquots of samples from the above extractions were silylated with 100 μl of N-methyl-N-(trimethylsilyl) trifluoroacetamide (MSTFA) with 1% trimethylchlorosilane (TMCS) at 60 °C for 40 min. The silylated samples were analyzed using an Agilent 7980 A gas chromatography (GC) system coupled to a 5975 C Series mass detector (Agilent Technologies, Santa Clara, CA, USA). Detailed GC-MS operating conditions are provided in Supporting information. Individual compounds were identified based on the comparison of mass spectra with literature, NIST library data, authentic external standards, and interpretation of mass spectrometric fragmentation patterns (Otto and Simpson, 2007; Feng et al., 2010; Tamura and Tharayil, 2014). Compounds were quantified based on external calibration curves using authentic standards (14 phenolic compounds for lignin monomers, sterol mixtures for phytosterol, 1-octadecanol for alkanols, 1-tetradecanoic acid for alkanoic acid, and 16-hydroxyhexadecanoic acid for hydroxy-alkanoic acids) in the total ion chromatogram (TIC). The concentration of individual compounds was normalized to the SOC content to reflect its relative abundance in SOC.

Amino sugars: Amino sugars are key components of microbial cell walls and can be used as a time-integrated microbial biomarker to indicate the contribution of microbial residue to SOC pools (Liang and Balser, 2012; Joergensen, 2018). Soil amino sugars mainly include muramic acid (MurA), glucosamine (GluN), and galactosamine (GalN). MurA originates exclusively from bacteria, whereas GluN originates from both fungi and bacteria (Amelung et al., 2001; Joergensen, 2018). The origin of soil GalN is uncertain, generally considered to be derived from bacteria, but also present in the cell walls of some rare archaeal species (Joergensen, 2018). These three amino sugars were determined using a method modified from Appuhn et al. (2004) and Olofsson and Bylund (2016). Briefly, 0.5 g of air-dried soil was hydrolyzed with 10 ml of 6 M HCl at 105 °C for 6 h. After cooling, the acid hydrolysate was filtered through a 0.45 μm membrane filter (Whatman GF/A). A 0.3-ml aliquot was evaporated to dryness at 40 °C to remove HCl, re-dissolved in 0.3 ml water, evaporated to dryness again, and finally re-dissolved in 1 ml of acetonitrile: ultrapure water (1: 1). After centrifuging at 7000 g, the supernatant was transferred to a GC vial and stored at −20 °C until analysis.

The amino sugars were identified based on accurate mass (<5 ppm error) and structural fragmentation of parent ions by collision-induced dissociation (CID) with argon. Following identification, amino sugars were quantified with an ultra-fast liquid chromatography coupled to a triple-quadrupole mass spectrometer (LCMS 8030; Shimadzu Scientific, Columbia, MD, USA) with an ESI interface (see detailed LC-ESI-MS/MS conditions in Supporting information). Before this analysis, multiple reaction monitoring (MRM) was optimized for the three amino sugars, with the final analyte m/z transition of (251.85 → 233.95, 216.00, 125.95), (179.90 → 161.95, 163.00, 72.05), and (179.90 → 162.10, 163.05, 72.15) for muramic acid, glucosamine, and galactosamine, respectively. Both the identities and quantities of these amino sugars were confirmed using commercially authentic standards (Muramic acid, D-glucosamine hydrochloride, and D-galactosamine hydrochloride).

Bacterial residue C was calculated by multiplying the concentration of MurA by 45, where 45 is the conversion value of MurA to bacterial residue C. Fungal residue C was calculated by subtracting bacterial GluN from total GluN, assuming that MurA and GluN on average occur at a 1–2 M ratio in bacterial cells. Fungal residue C = (mmol GluN − 2 × mmol MurA) * 179.17 * 9, where 179.17 is the molecular weight of GluN and 9 is the conversion value of fungal GluN to fungal residue C. Microbial residue C was the sum of fungal residue C and bacterial residue C (Joergensen, 2018; Liang et al., 2019). The ratios of GluN/MurA and GluN/GalN were used as indicators to track the relative contribution of fungi and bacteria to microbial residues in soil (Liang et al., 2013).

2.3. Soil microbial community composition

The soil microbial community was characterized by phospholipid fatty acid (PLFA) analysis using a modified method according to Bossio and Scow (1998), Quideau et al. (2016), and Jatana et al. (2020). Briefly, the lipids in 5 g of fresh soil were extracted with a one-phase mixture of chloroform, methanol, and citrate buffer (1:2:0.8, v/v/v). The extract containing fatty methyl esters was analyzed using an Agilent 7980 A GC system coupled to a 5975 C Series mass detector (Agilent Technologies, Santa Clara, CA, USA; see detailed extraction protocols and GC-MS operating conditions in Supporting information). Individual PLFAs were identified by the comparison of mass spectra with literature and NIST library data. PLFAs were quantified by comparing the peak areas of the samples with the peak areas of the internal standard (heneicosanoic methyl ester; $C_{21:0}$) of a known concentration, which were expressed in nmol PLFA/g dry soil. Microbial biomass was calculated by summarizing total PLFAs (C_{14}–C_{20}). PLFAs specific to Gram-negative bacteria (16:1ω7c, cy17:0 and cy19:0), Gram-positive bacteria (i14:0, a15:0, i16:0, i17:0 and a17:0), fungi (18:2ω6, 9c and 18:1ω9c), and actinomycetes (10Me17:0 and 10Me18:0) were summarized, respectively. The composition of soil microbial community was assessed by the ratios of Gram-negative to Gram-positive bacterial PLFAs (G^-/G^+) and fungal PLFAs to bacterial PLFAs (the sum of G^- and G^+ bacterial PLFAs (Baath and Anderson, 2003; Schindlbacher et al., 2011);).

2.4. Statistical analysis

The Shapiro-Wilk test showed that all data were normally distributed. To compare the effect of treatments on the concentration of SOC components (lipids, phytosterol, lignin monomers, and amino sugars) and soil PLFA concentrations, one-way analysis of variance (ANOVA) was used, followed by a post-hoc Tukey's HSD multiple comparison test using the "multcomp" package in R (R Core Team, 2018). Statistical tests were considered significant at the $P < 0.05$ level. The principal component analysis (PCA) was used to visualize the differences in SOC chemical composition of the normalized concentration data (mg g^{-1} SOC) for 6 groups of biomarkers (Bodmer et al., 2016). The nonmetric multidimensional scaling (NMDS) analysis was used to visualize the microbial community structure patterns, based on the Bray–Curtis dissimilarity (distance) of the variability of the normalized abundance data (mole-percent) for 20 PLFAs (Borcard et al., 2018). The PERMANOVA was performed with 999 permutations to further test the differences using the adonis function of the R vegan package (Oksanen et al., 2013).

3. Results

3.1. Quantity and chemical composition of litter inputs

The accumulated litter biomass in the knotweed-invaded pots was around 50% lower compared with the noninvaded pots that were dominated by grass species ($P < 0.05$; Table 1). The C: N ratio of knotweed litter was 90% higher than the litter in the noninvaded pots ($P < 0.05$; Table 1). Compared with the litter in the noninvaded pots, the knotweed litter in the invaded pots had 40% and 3-times higher lignin and tannins per unit biomass, respectively ($P < 0.05$), while there was no difference in the concentration of lipids ($P > 0.05$). In addition, the knotweed litter had a higher ratio of $(Ad/Al)_s$ than the litter in the noninvaded pots ($P < 0.05$; Table 1).

Fertilizer application increased the accumulated litter biomass by 44%, while reduced the litter C: N ratio by 25% in the invaded pots ($P < 0.05$; Table 1). Compared with the unfertilized knotweed litter, litter in

Table 1
Characteristics of litter inputs in the noninvaded, invaded, and invaded + fertilized pots.

	Noninvaded	Invaded	Invaded + Fertilized
Accumulated litter (g m^{-2})[a]	3075.56 (613.78)[a]	1686.66 (126.66)[b]	2428.88 (298.22)[a]
Litter C/N ratio	67.1 (20.3)[b]	126.3 (15.4)[a]	94.5 (10.6)[b]
Biomass lipids (%)	0.49 (0.05)[b]	0.55 (0.04)[b]	0.72 (0.06)[a]
Biomass lignin (%)	2.39 (0.35)[c]	3.24 (0.14)[ab]	3.44 (0.18)[a]
Biomass tannin (%)	0.23 (0.02)[b]	0.95 (0.06)[a]	0.95 (0.07)[a]
$(Ad/Al)_s$	0.19 (0.004)[a]	0.15 (0.007)[a]	0.16 (0.01)[a]
$(Ad/Al)_v$	0.21 (0.03)[a]	0.20 (0.01)[a]	0.22 (0.02)[a]

Each value represents the ±1 SE of the mean (n = 5 for the noninvaded treatment; n = 8 for the invaded treatment; n = 7 for the invaded + fertilized treatment). Different lowercase letters within a row denote significant differences among treatments at $P < 0.05$.

[a] Quantified as the accumulated litter biomass by harvesting litter layer in a 0.0225-m^2 area within the sampling pots.

the fertilized pots had 31% higher lipids per unit biomass ($P < 0.05$), but had no difference in the concentrations of lignin and tannins ($P > 0.05$). The ratio of $(Ad/Al)_s$ or $(Ad/Al)_v$ in the knotweed litter did not differ between the fertilized and the unfertilized treatment ($P > 0.05$; Table 1).

3.2. Molecular composition of SOC in the mineral soil

The knotweed-invaded soils did not differ from the noninvaded soils with respect to the bulk SOC content ($P > 0.05$; Table 2). The SOC content in the invaded soils increased marginally with fertilizer application ($P = 0.066$; Table 2). Changes in the entire molecular profile of SOC were identified using PCA analysis of biomarkers across different treatments, which accounted for a total of 72.7% of the variance of the SOC chemical compositions (Fig. 1). The invaded and noninvaded soils did not clearly separate according to the treatments ($P > 0.05$; Fig. 1), while the invaded and the invaded + fertilized soils were scattered along axis 2 with the concentrations of long-chain fatty acids, phytosterol, lignin monomers, and amino sugars accounting for most of the variations ($P < 0.01$; Fig. 1).

Solvent extractable lipids and sterols: The amount of solvent extractable lipids in the soil was not influenced by knotweed invasion, including long-chain fatty acids and cutin- and suberin-derived lipids ($P > 0.05$; Fig. 2a). However, the knotweed-invaded soils exhibited a 50% increase in the concentration of phytosterol compared with the noninvaded soils ($P < 0.01$; Fig. 2a). Fertilized soils had higher concentrations of long-chain fatty acids and phytosterol ($P < 0.01$), while fertilizer application did not affect cutin and suberin concentrations in the invaded soils ($P > 0.05$; Fig. 2a).

Lignin monomers: Similar to the solvent-extractable lipids, the concentrations of total CuO oxidation products and total lignin monomers (SVC) did not show differences between the invaded and noninvaded soils ($P > 0.05$; Fig. S2; Fig. 2b). Compared with the unfertilized soils, the invaded soils after fertilizer application exhibited a 25% increase in the concentration of lignin monomers ($P < 0.05$; Fig. 2a). The ratios of acid to aldehyde lignin in syringyl and vanillyl based monomers [$(Ad/Al)_s$ and $(Ad/Al)_v$] in the invaded soils were generally higher than those in the noninvaded soils; however, this trend was not significant ($P > 0.05$; Fig. 2c and d). Fertilizer application increased the ratio of both $(Ad/Al)_s$ and $(Ad/Al)_v$ in the invaded soils ($P < 0.05$; Fig. 2c and d).

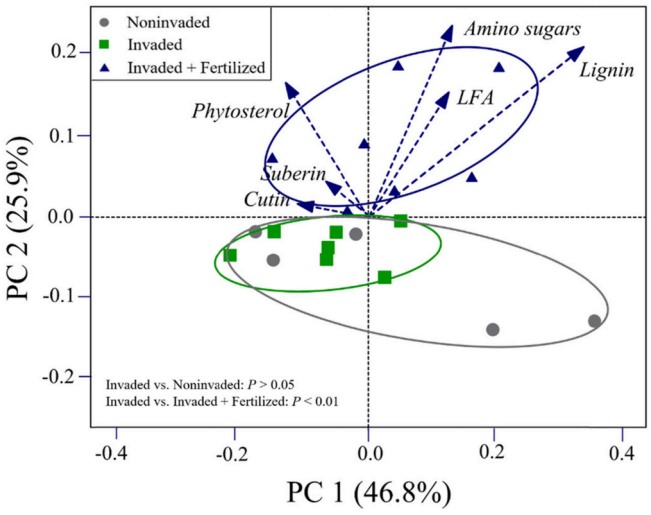

Fig. 1. Results of the principal component analysis (PCA) of different SOC chemical compositions based on the normalized concentration of 6 groups of compounds. Continuous lines enclose different treatment groups. Axis 1 and axis 2 represent the explained percentage of the variance. PERMANOVA was used to test the differences in the SOC compositions between the invaded and noninvaded treatments, and between the invaded and invaded + fertilized treatments, separately. Dotted arrows indicate variable loadings which reveal the directions and strength of the variations of these chemical compounds along each axis. *Gray dots, green squares*, and *blue triangles* represent the noninvaded, invaded, and invaded + fertilized treatment, respectively. LFA, long-chain fatty acids (>C_{24} alkanes, > C_{22} n-alkanoic acids and alkanols); Cutin, (C_{14}–C_{18} hydroxyalkanoic acids, C_{16}-di-hydroxyalkanoic acids, ω-hydroxy- and ω-hydroxy-epoxy alkanoic acids (C_{16}–C_{18})); Suberin, (α,ω-dicarboxilic acids (C_{16}–C_{24}; saturated and substituted) and ω-hydroxyalkanoic acids (C_{20}–C_{30}; saturated and substituted)). (For interpretation of the references to color in this figure legend, the reader is referred to the Web version of this article.)

Amino sugars: The amount of total amino sugars in the invaded soils was higher than the noninvaded soils, which was mainly attributed to a 20% increase in the concentration of GluN ($P < 0.05$; Fig. 3a). No differences were observed for the concentrations of MurA and GlaN between the invaded and noninvaded soils ($P > 0.05$; Fig. 3a). Fertilizer application increased the concentrations of MurA, GluN, and GlaN in the invaded soils by 46.2%, 18.4%, and 18.3%, respectively, contributing to a 19.4% increase in the concentrations of total amino sugars ($P < 0.05$; Fig. 3a). Compared with the noninvaded soils, the invaded soils exhibited a marginally higher GluN/MurA ratio ($P = 0.059$); in contrast, the invaded soils following fertilizer application showed a lower GluN/MurA ratio ($P < 0.05$; Fig. 3b). Differences in GluN/GalN ratio were neither observed between the invaded and noninvaded soils nor between invaded and invaded + fertilized soils ($P > 0.05$; Fig. 3c). The invasion of knotweed significantly increased the contribution of fungal residue C to the SOC pool but did not change the proportion of bacterial residue C ($P > 0.05$; Fig. S3). Fertilizer application enhanced the contributions of both fungal and bacterial residue C to the SOC pool in the invaded soils ($P < 0.01$; Fig. S3).

Table 2
Characteristics of soils in the noninvaded, invaded, and invaded + fertilized pots.

	Noninvaded	Invaded	Invaded + Fertilized
pH[a]	5.8 (0.3)[a]	6.1 (0.5)[a]	5.3 (0.4)[a]
SOC (mg g^{-1})	13.91 (0.88)[b]	15.79 (0.95)[a]	18.42 (0.89)[a]
Total N (mg g^{-1})	1.49 (0.10)[b]	1.59 (0.09)[b]	1.90 (0.08)[a]
C/N ratio	9.36 (0.40)[a]	9.88 (0.09)[a]	9.66 (0.09)[a]
DIN (μg g^{-1})	75.28 (6.33)[a]	45.33 (3.17)[b]	65.85 (2.72)[a]
DON (μg g^{-1})	169.05 (15.83)[b]	241.48 (11.52)[a]	202.44 (20.74)[a]
DIN/DON ratio	0.44 (0.10)[a]	0.19 (0.03)[b]	0.32 (0.03)[a]

Each value represents the ±1 SE of the mean (n = 5 for the noninvaded treatment; n = 8 for the invaded treatment; n = 7 for the invaded + fertilized treatment). Different lowercase letters within a row denote significant differences among treatments at $P < 0.05$. Key: DIN, Dissolved inorganic N; DON, Dissolved organic N.

[a] Measured in 1: 2.5 of soil: water suspensions with a pH electrode.

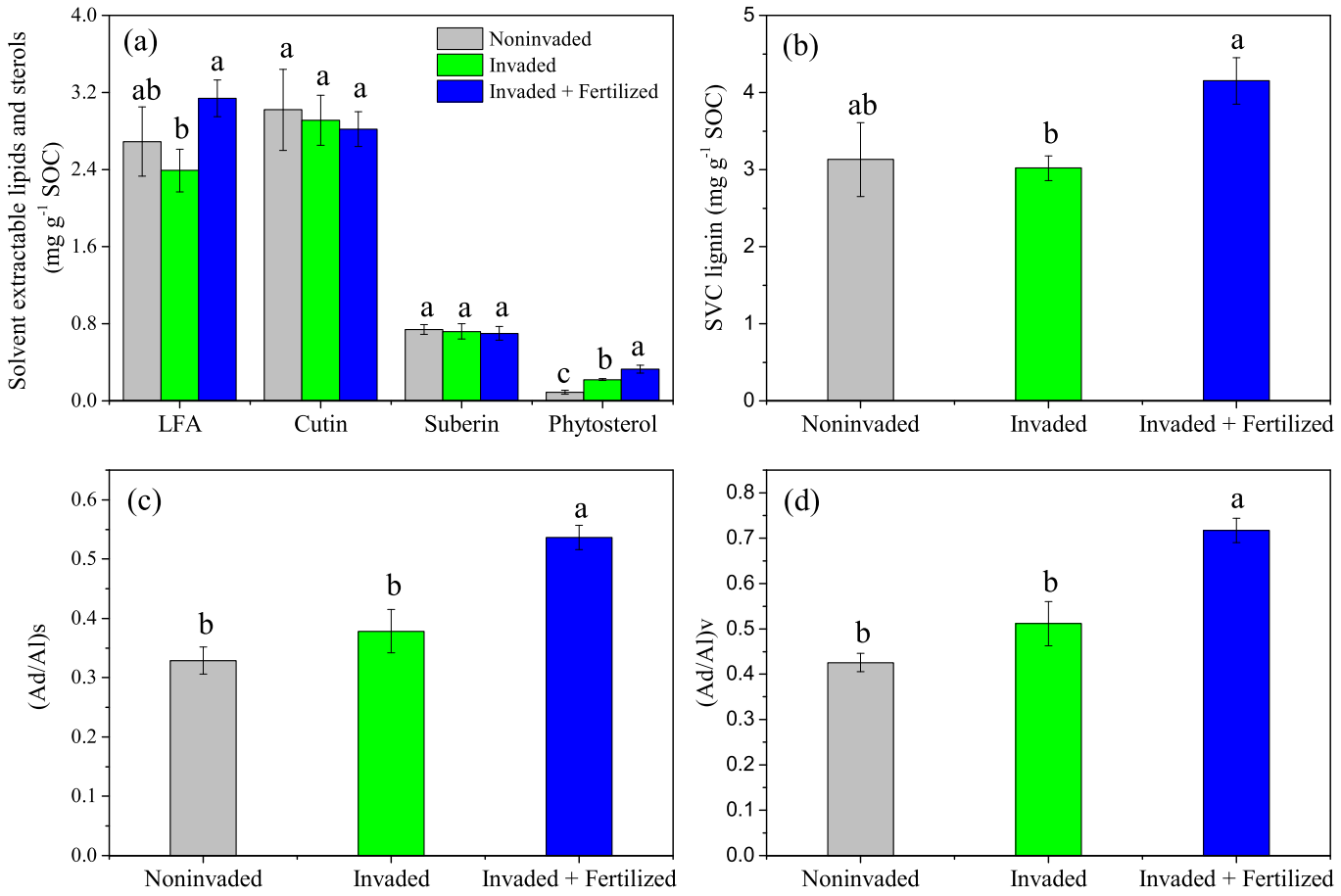

Fig. 2. Concentration of solvent extractable lipids and sterols (a), concentration of lignin monomers (b), and degradation parameters of lignin (c–d) after CuO oxidation in the mineral soils (0–15 cm) under the noninvaded, invaded, and invaded + fertilized treatments. SVC: S = Syringyls (syringaldehyde, acetosyringone, and syringic acid); V = Vanillyls (vanillin, acetovanillone, and vanillic acid); C = Cinnamyls (p-coumaric acid and ferulic acid). (Ad/Al)s: ratio of syringic acid/syringaldehyde. (Ad/Al)v: ratio of vanillic acid/vanillin. Error bars are ±1SE of the mean (n = 5 for the noninvaded treatment; n = 8 for the invaded treatment; n = 7 for the invaded + fertilized treatment) with lowercase letters above bars indicating significant differences among treatments at $P < 0.05$.

3.3. Soil microbial community composition

Both invasion of knotweed and fertilizer application affected the composition of the soil microbial community, which were summarized by the NMDS analysis (Fig. 4) and the treatment effects on the concentration of individual PLFAs (Table 3). In the NMDS analysis, the invaded and the invaded + fertilized soils separated along axis 1 (explaining 67.2% of the variation in the PLFA data), while no clear separation was observed between the invaded and noninvaded soils along axis 1 (Fig. 4). Fertilized soil was positively associated with the fungal markers (18:2ω6, 9c and 18:1ω9c), G^+ bacterial markers (i14:0, i16:0 and a17:0), and actinomycete markers (10Me17:0 and 10Me18:0) (Fig. 4). The total PLFA concentrations showed a marginal increase in the knotweed-invaded soils compared with the noninvaded soils ($P = 0.06$; Table 3). The fertilizer application treatment further increased the total PLFA biomass in the invaded soils ($P < 0.05$; Table 3). For individual PLFAs, compared with the noninvaded soils, significantly higher PLFA concentrations were observed only for fungi in the invaded soils. Fertilizer application increased all groups of PLFAs except G^- bacteria in the invaded soils ($P < 0.05$; Table 3). In addition, the G^+/G^- ratio was higher in the fertilized soils ($P < 0.05$; Table 3).

4. Discussion

Although it is becoming increasingly evident that plant invasion has a dramatic influence on the cycling and stocks of soil C stocks due to altered vegetation types, relatively few studies have attempted to investigate the effects of plant invasion on the chemical composition of SOC pools at the molecular level (Tamura and Tharayil, 2014; Li et al., 2017), and particularly how these effects respond to altered N availability since N deposition is another major global change factor that can interact with plant invasion. In this study, while only minor changes in the total SOC content were observed, the results from this mesocosm experiment suggested that the invasion of Japanese knotweed primarily altered the proportion of microbial-derived C in SOC pools. Among the plant-derived C, only the concentrations of phytosterol were higher in the invaded soils compared with the noninvaded soils. In addition, fertilizer application significantly increased both plant- and microbial-derived C components in the knotweed-invaded soils. These endogenous changes to SOC composition may have important implications for soil C sequestration and long-term feedbacks on plant invasions and climate change.

4.1. Altered SOC chemical composition following knotweed invasion

Most invasive plants often have chemically distinct litter (both roots and leaves) compared with native plant species (Liao et al., 2008), which may potentially alter the chemical composition of SOC (Tamura and Tharayil, 2014; Tamura et al., 2017). We hypothesized that the input of low-quality litter (i.e., high recalcitrance with low metabolic compounds) from knotweed would increase the concentration of plant-derived C in the invaded soils. Contrary to our expectation, despite the knotweed-invaded soils received leaf litter which was abundant in lignin and tannins compared with litter in the noninvaded treatments

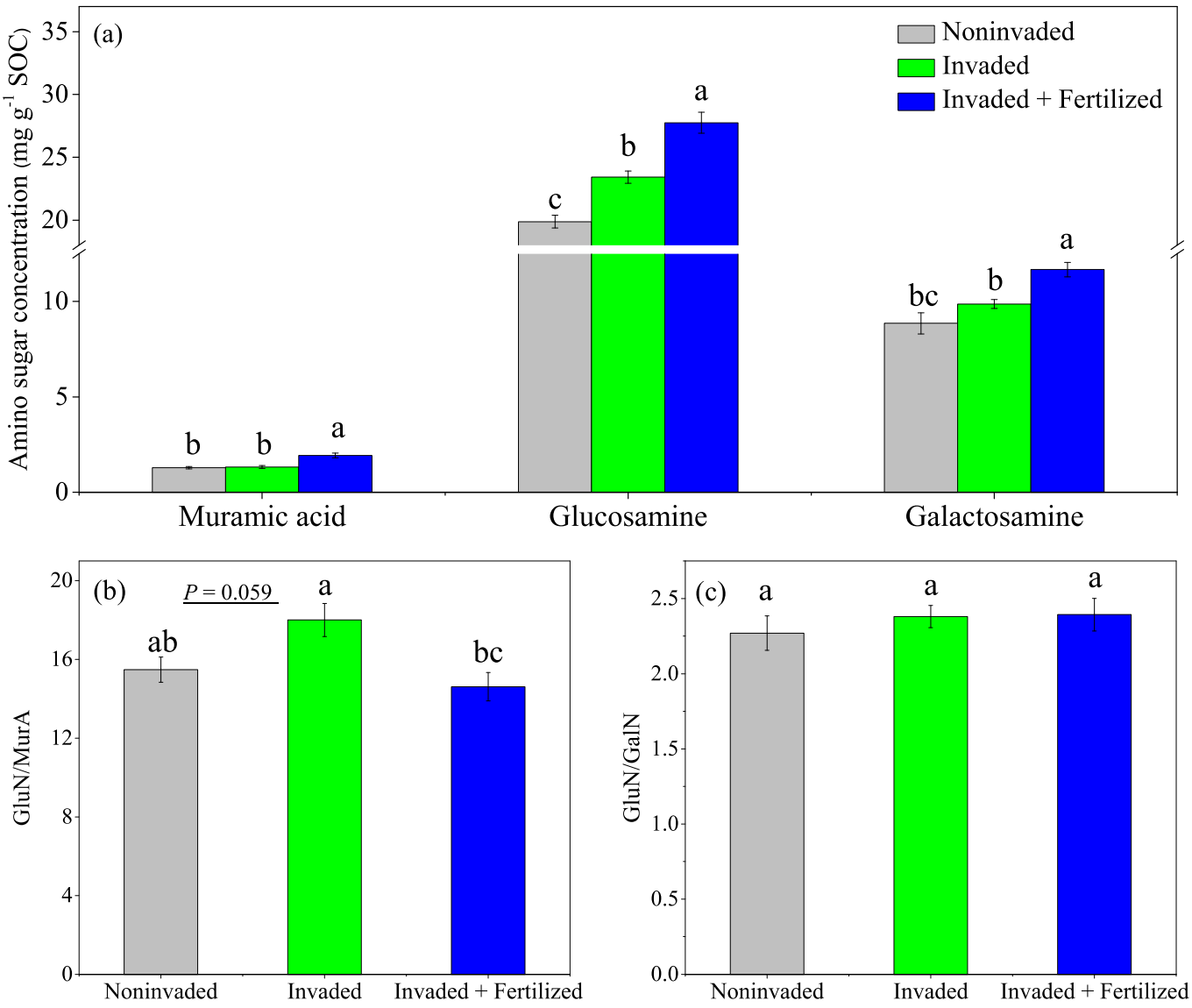

Fig. 3. Concentration of muramic acid, glucosamine, and galactosamine (a) and ratios of glucosamine to muramic acid (GluN/MurA) (b) and glucosamine to galactosamine (GluN/GalN) (c) in the mineral soils (0–15 cm) under the noninvaded, invaded, and invaded + fertilized treatments. Error bars are ±1SE of the mean (n = 5 for the noninvaded treatment; n = 8 for the invaded treatment; n = 7 for the invaded + fertilized treatment) with lowercase letters above bars indicating significant differences among treatments at $P < 0.05$.

(Table 1), most of the plant-derived compounds such as long-chain fatty acids, suberin, cutin, and lignin monomers, except phytosterol, exhibited similar abundance between the invaded and noninvaded mineral soils (Fig. 2a and b). This result is inconsistent with the reported higher retainment of plant recalcitrant lipids and phenolics in the knotweed-invaded soils from our previous studies under field conditions where knotweed has been invaded for >20 years (Tamura and Tharayil, 2014; Suseela et al., 2016). This undetected difference of plant biomarkers in the soil following the invasion of knotweed in this study could be potentially due to the lower litter input in the invaded soils albeit greater recalcitrance of knotweed litter (Table 1), which yielded an equivalent abundance of plant-derived compounds between the invaded and noninvaded soils. During soil and litter sampling, the surface litter accumulation in the noninvaded pots inhabited by grasses was 2-fold higher than that in the knotweed-invaded pots (Table 1), due to the high density of grass species in the noninvaded soils. In addition, the similar content of plant biomarkers between the noninvaded and invaded treatments is also likely to be attributed to the higher root distribution of grass species at the sampling depth in the noninvaded soil (field observation with data not shown). Previous research has indicated that in Japanese knotweed under field conditions had 50% and 25% lower root biomass at 5–10 and 10–15 cm depths, respectively, compared with the adjacent non-invaded soils inhabited by grasses and forbs (Tamura and Tharayil, 2014). It should be noted that the persistent effect of plant invasion on soil chemistry usually occurs in sites that are dominated by invasive species for many years where the litter input from the invasive species far exceeds the litter input by the native plant community. Thus, the litter (both above- and below-ground) input by knotweed growing in the present pot experiment may not be representative of the litter input in the long-standing knotweed-invaded sites under natural conditions. Litterfall of knotweed was constrained in this experiment due to the relatively short growing period and hence the lower plant biomass. Besides the difference in the litter accumulation between the invaded and noninvaded soils, a potential explanation for the less dramatic effects of invasion on soil C chemistry in the present study could be that we used 0–15 cm of soil for our analyses (Dornbush, 2014; Tautges et al., 2019). In a previous study, it was reported that the selective preservation of plant-derived compounds due to knotweed

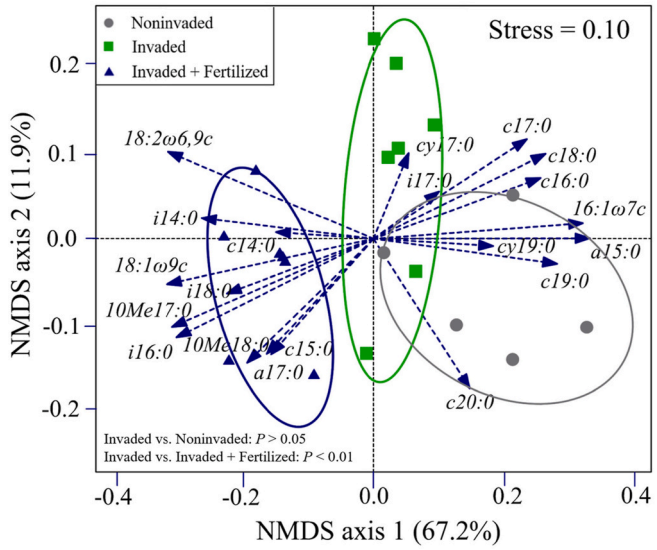

Fig. 4. Results of a nonmetric multidimensional scaling (NMDS) ordination of microbial community composition based on transformed abundances of 20 PLFA biomarkers. Continuous lines enclose different treatment groups. Axis 1 and axis 2 represent the explained percentage of the variance. PERMANOVA was used to test the differences in the microbial community compositions between the invaded and noninvaded treatments, and between the invaded and invaded + fertilized treatments, separately. Dotted arrows denote significant correlations (Pearson) between ordination scores and microbial biomarkers ($P < 0.05$). *Gray dots, green squares*, and *blue triangles* represent the noninvaded, invaded, and invaded + fertilized treatment, respectively. (For interpretation of the references to color in this figure legend, the reader is referred to the Web version of this article.)

Table 3
Soil microbial phospholipids acid (PLFA) biomarkers contents (nmol g^{-1} soil) in the mineral soils (0–15 cm) under the noninvaded, invaded, and invaded + fertilized treatments.

	Noninvaded	Invaded	Invaded + Fertilized
Total PLFA	55.44 (5.71)^{b}	68.73 (3.42)^{b}	86.67 (2.66)^{a}
Fungi	7.82 (0.42)^{c}	10.46 (0.88)^{b}	14.04 (0.96)^{a}
Bacteria	26.60 (2.73)^{b}	31.38 (1.58)^{b}	40.69 (1.18)^{a}
G^{+}	15.12 (1.56)^{b}	18.02 (1.12)^{b}	25.65 (0.89)^{a}
G^{-}	11.47 (1.18)^{bc}	13.36 (0.57)^{ab}	15.03 (0.52)^{a}
Actinomycetes	3.41 (0.42)^{bc}	4.00 (0.30)^{ab}	5.80 (0.20)^{a}
Fungi/Bacteria	0.29 (0.02)^{a}	0.33 (0.02)^{a}	0.34 (0.02)^{a}
G^{+}/G^{-}	1.32 (0.03)^{b}	1.35 (0.06)^{b}	1.71 (0.07)^{a}

Each value represents the ±1 SE of the mean (n = 5 for the noninvaded treatment; n = 8 for the invaded treatment; n = 7 for the invaded + fertilized treatment). Different lowercase letters within a row denote significant differences among treatments at $P < 0.05$. Key: G^{+}, Gram positive; G^{-}, Gram negative.

litter input was limited to the 0–5 cm soil layer in the knotweed-invaded stands (Tamura and Tharayil, 2014). Thus, it is plausible to assume that the detection of significant changes in plant-derived compounds following knotweed invasion might be hindered when profiling the entire 0–15 cm soil depth due to the decreased vertical transport of altered surface SOC with an increase in soil depth.

Besides plant-derived aliphatic structures, microbial-derived C inputs to soils are increasingly recognized to contribute to the stabilization of SOC (Appuhn et al., 2006; Liang et al., 2017). In comparison to the plant-derived compounds, a substantial amount of microbial residue C as indicated by amino sugars was retained in the knotweed-invaded soils (Fig. 3a; Fig. S3), a result contrary to our predictions. The greater abundance of microbial residue C mostly resulted from the increased soil fungal community and subsequent accumulation of fungal necromass following knotweed invasion. This observation was further supported by the observed trend of a greater ratio of GluN/MurA (Fig. 3b) and increased fungal biomass as indicated by PLFAs in the invaded soils (Table 3). Similar greater fungal biomass has been reported due to the higher abundance of plant secondary metabolites (e.g., phenolic compounds) that persisted in the knotweed-invaded soils (Tamura and Tharayil, 2014; Suseela et al., 2016). A plausible explanation could be that the high inputs of tannin (Table 1) and other phenolics derived from the litter of knotweed increased the abundance of fungi (slow decomposers adapted to phenol-rich conditions) relative to bacteria (fast decomposers) (Mutabaruka et al., 2007). Further examination of the contribution of dominant polyphenolic compounds to soil C cycling and sequestration in the invaded soils, via impacting soil microbial biomass and community composition, would be a worthwhile focus of future studies.

4.2. *Fertilizer application-induced changes in SOC composition and degradation in the invaded soils*

Consistent with our hypothesis, plant-derived compounds (plant lipids and lignin monomers) were significantly enriched in the knotweed-invaded mineral soils after a decade of experimental fertilizer application (Fig. 2; Fig. S2). This result was coincident with the preservation of plant-derived recalcitrant structures in the soil under fertilizer application as reported in previous studies (Zak et al., 2008; Feng et al., 2010; Frey et al., 2014). Soil C accrual and chemical composition are affected by both the C input (litterfall and root biomass turnover) and output (C losses from litter and soil organic matter decomposition) processes (Frey et al., 2014). Fertilizer application promotes plant growth and net primary productivity in nutrient-limited conditions (Oren et al., 2001; LeBauer and Treseder, 2008), and subsequently elevates plant-derived C inputs from leaf litter and roots. Our results showed that fertilizer application stimulated the growth of knotweed (field observation) and increased the inputs of leaf litter with enriched undecomposed plant lipids in the knotweed-invaded soils (Table 1). Greater litter inputs induced by fertilizer application might facilitate the persistence of plant-derived compounds in the soil (Feng et al., 2010). Although we did not measure root biomass or inputs in the present study, results from a meta-analysis have shown that nutrient addition tends to increase fine root production (Yuan and Chen, 2012). In addition, fertilizer application (e.g., N addition) could promote SOC accumulation through decreasing litter C: N ratio (Fornara and Tilman, 2012; Ziter and MacDougall, 2013), which was also evident in this study (Table 1). Plant litter with a lower C: N ratio could accelerate the physical incorporation of plant-derived recalcitrant C into the soil matrix (Zhou et al., 2019). Apart from increasing SOC through enhanced plant biomass and lowered litter C: N ratio, a suppression of organic matter decay in response to nutrient addition has been considered as an alternative mechanism leading to the accumulation of recalcitrant compounds such as lignin in the soil (Pregitzer et al., 2008; Zak et al., 2008, 2019). Many studies have reported that fertilizer application, especially N addition, could inhibit the degradation of lignin by suppressing the synthesis of lignolytic enzymes, thus contributing to the increase of soil lignin (Waldrop et al., 2004; Treseder, 2008; Zak et al., 2008). It is noteworthy that fertilizer application enhanced lignin oxidation (indicated by the increased ratio of $(Ad/Al)_s$ and $(Ad/Al)_v$) in the knotweed-invaded soils (Fig. 2c and d), which was contrary to our prediction and most previous studies. This observation may be attributed to the changed soil microbial activities and community composition following fertilizer application (Feng et al., 2010). Our results also showed that fertilizer application significantly increased fungal biomass in the knotweed-invaded soils (Table 3), which may stimulate the degradation of soil lignin. The detected higher fungal biomass in this study was further supported by the higher content of ergosterol in the soil (Fig. S5). Both positive and negative responses of soil fungal biomass to fertilizer application have been reported, depending on organic matter chemistry and nutrient status at specific systems (Treseder, 2008;

Weand et al., 2010; Griepentrog et al., 2014). We interpret the increase of fungal biomass and activities in the knotweed-invaded soils as a response to accumulated plant-derived recalcitrant compounds following fertilizer application rather than a direct effect induced by fertilizer application. Increased fraction of recalcitrant compounds results in less C availability to some soil microbes but would enhance microbial species specializing in the utilization of these compounds (Liu et al., 2016). Consistently, fertilizer application in the knotweed-invaded soils significantly increased the biomass of actinomycetes and G^+ bacteria (Table 3) which also harbor certain abilities to solubilize lignin and low-quality substrates (Eisenlord et al., 2013; Fanin et al., 2019). Overall, our results indicated that the accumulation of plant-derived C in the knotweed-invaded soils in response to fertilizer application was largely due to the enhanced C input processes over C output processes.

Similar to the response of plant-derived C components, fertilizer application positively affected the accumulation of microbial residue in the knotweed-invaded soils. Greater retention of soil amino sugars under fertilizer application may be caused by the active assimilation of plant-derived C into microbial biomass, which eventually formed stabilized SOC through *in vivo* turnover processes and preferential retention of microbial byproducts (Liang et al., 2017). This interpretation could be corroborated by the increased microbial C-use efficiency (decreased microbial metabolic quotient; defined as the fraction of C uptake allocated to microbial growth and biosynthesis) under fertilizer application (Fig. S4b). Soil microbial C-use efficiency has been suggested to increase in response to increasing inorganic N supply when the microbes are N-limited (Ziegler and Billings, 2011; Manzoni et al., 2012). Our results showed that fertilizer application increased N availability in the knotweed-invaded soils (greater ratio of DIN/DON in Table 2), thus might relieve soil microbes from conditions of N limitation and increase their C-use efficiency (Ziegler and Billings, 2011). As discussed above, although recalcitrant plant-derived C inputs into soil increased with fertilizer application, it could stimulate anabolic activities of certain groups of soil microorganisms such as fungi which are recognized as more efficient in substrate use than bacteria (Strickland and Rousk, 2010). Given that fertilizer application had minimal impact on soil basal respiration in the knotweed-invaded soils in the present study (Fig. S4a), the higher microbial residues, therefore, imply that soil microbes tend to invest more C in anabolism than catabolism. Alternatively, the relatively lower accumulation of microbial residues in unfertilized soils might result from the increased degradation of amino sugars. It has been suggested that soil microbes preferentially decompose residues from their cell walls rather than accumulating biomass, when available C and N become limited (Amelung et al., 2001; Ding et al., 2010). Despite the increased concentrations of individual amino sugars and the size of total amino sugar pool, fertilizer application did not significantly alter the relative contribution of fungi and bacteria to microbial residues in the knotweed-invaded soils (Fig. S3). This was consistent with the unchanged biomass ratios of fungi to bacteria under fertilizer application (Table 3), while this was in contrast with the significant decrease in GluN/MurA ratios (Fig. 3b) which indicates a lower fungal contribution to microbial residues in fertilized soils. The decreased ratios of GluN to MurA following N addition could be simply explained and confirmed by a shift in the bacterial community towards G^+ bacteria, as G^- bacteria contain a thinner murein layer, thus leading to much lower MurA than G^+ bacteria (Appuhn et al., 2006; Joergensen, 2018). Our results suggest that the microbial contribution to SOC pools is closely related to microbial biomass and community dynamics.

5. Conclusion and implications

Although short-term manipulation experiments based on planting invasive plants do not realistically reflect the field conditions due to their short duration, lower plant biomass, and litter deposition, they can mirror an early stage of the establishment of the exotic plants in disturbed bare soil with vegetation temporally absent. These experiments could be considered complementary to observational field studies where site history and invasion effect could be confounded. The results of this study provide molecular-level evidence that plant invasion significantly influences the chemical composition of SOC, even where the difference in respiration or total SOC content is not apparent. Given that these effects were primarily observed on microbial-derived C and not on plant-derived C, our results highlight the greater sensitivity of soil microbial anabolism and community dynamics to plant invasion. Moreover, our results demonstrate that fertilizer application reinforces the effects of plant invasion on the composition and accrual of SOC via accelerating the inputs and accumulation of both plant-derived and microbial-derived C in the soil. As plant invasion is predicted to rapidly expand with increasing N deposition, the dramatically altered dynamics of SOC composition in response to plant invasion under fertilizer application have ecologically important implications for the restoration of the invaded ecosystems. Considering the uncertainty as to how invasive plants respond to other components of global change acting alone or in concert, our findings also suggest the need to further understand the impacts of biological invasion in the context of other major or interacting global change drivers that act to both affect invasion and modulate their effects.

Declaration of competing interest

The authors declare that they have no known competing financial interests or personal relationships that could have appeared to influence the work reported in this paper.

Acknowledgments

The research was based on work that is supported by the U.S. Department of Agriculture, National Institute of Food and Agriculture (USDA/NIFA), United States (project number 2017-67014-26698). This is a technical contribution No. 6953 of the Clemson University Experimental Station.

Appendix A. Supplementary data

Supplementary data to this article can be found online at https://doi.org/10.1016/j.soilbio.2021.108195.

References

Amelung, W., Miltner, A., Zhang, X., Zech, W., 2001. Fate of microbial residues during litter decomposition as affected by minerals. Soil Science 166, 598–606.
Angst, G., Mueller, K.E., Kogel-Knabner, I., Freeman, K.H., Mueller, C.W., 2017. Aggregation controls the stability of lignin and lipids in clay-sized particulate and mineral associated organic matter. Biogeochemistry 132, 307–324.
Appuhn, A., Joergensen, R.G., Raubuch, M., Scheller, E., Wilke, B., 2004. The automated determination of glucosamine, galactosamine, muramic acid, and mannosamine in soil and root hydrolysates by HPLC. Journal of Plant Nutrition and Soil Science 167, 17–21.
Appuhn, A., Scheller, E., Joergensen, R.G., 2006. Relationships between microbial indices in roots and silt loam soils forming a gradient in soil organic matter. Soil Biology and Biochemistry 38, 2557–2564.
Baath, E., Anderson, T.H., 2003. Comparison of soil fungal/bacterial ratios in a pH gradient using physiological and PLFA-based techniques. Soil Biology and Biochemistry 35, 955–963.
Barney, J.N., Tharayil, N., DiTommaso, A., Bhowmik, P.C., 2006. The biology of invasive alien plants in Canada. 5. *Polygonum cuspidatum* Sieb. & Zucc. [= *Fallopia japonica* (Houtt.) Ronse Decr.]. Canadian Journal of Plant Science 86, 887–905.
Belay-Tedla, A., Zhou, X.H., Su, B., Wan, S.Q., Luo, Y.Q., 2009. Labile, recalcitrant, and microbial carbon and nitrogen pools of a tallgrass prairie soil in the US Great Plains subjected to experimental warming and clipping. Soil Biology and Biochemistry 41, 110–116.
Blumenthal, D., Chimner, R.A., Welker, J.M., Morgan, J.A., 2008. Increased snow facilitates plant invasion in mixedgrass prairie. New Phytologist 179, 440–448.
Bodmer, P., Heinz, M., Pusch, M., Singer, G., Premke, K., 2016. Carbon dynamics and their link to dissolved organic matter quality across contrasting stream ecosystems. The Science of the Total Environment 553, 574–586.

Borcard, D., Gillet, F., Legendre, P., 2018. Unconstrained Ordination, Numerical Ecology with R. Springer, pp. 151–201.
Bossio, D.A., Scow, K.M., 1998. Impacts of carbon and flooding on soil microbial communities: phospholipid fatty acid profiles and substrate utilization patterns. Microbial Ecology 35, 265–278.
Bradley, B.A., Blumenthal, D.M., Wilcove, D.S., Ziska, L.H., 2010. Predicting plant invasions in an era of global change. Trends in Ecology & Evolution 25, 310–318.
Brooks, M.L., 2003. Effects of increased soil nitrogen on the dominance of alien annual plants in the Mojave Desert. Journal of Applied Ecology 40, 344–353.
Cotrufo, M.F., Soong, J.L., Horton, A.J., Campbell, E.E., Haddix, M.L., Wall, D.H., Parton, A.J., 2015. Formation of soil organic matter via biochemical and physical pathways of litter mass loss. Nature Geoscience 8, 776–779.
Craig, M.E., Pearson, S.M., Fraterrigo, J.M., 2015. Grass invasion effects on forest soil carbon depend on landscape-level land use patterns. Ecology 96, 2265–2279.
Craig, M.E., Lovko, N., Flory, S.L., Wright, J.P., Phillips, R.P., 2019. Impacts of an invasive grass on soil organic matter pools vary across a tree-mycorrhizal gradient. Biogeochemistry 144, 149–164.
Dijkstra, F.A., Hobbie, S.E., Knops, J.M.H., Reich, P.B., 2004. Nitrogen deposition and plant species interact to influence soil carbon stabilization. Ecology Letters 7, 1192–1198.
Ding, X.L., Zhang, X.D., He, H.B., Xie, H.T., 2010. Dynamics of soil amino sugar pools during decomposition processes of corn residues as affected by inorganic N addition. Journal of Soils and Sediments 10, 758–766.
Ding, J.L., Jiang, X., Ma, M.C., Zhou, B.K., Guan, D.W., Zhao, B.S., Zhou, J., Cao, F.M., Li, L., Li, J., 2016. Effect of 35 years inorganic fertilizer and manure amendment on structure of bacterial and archaeal communities in black soil of northeast China. Applied Soil Ecology 105, 187–195.
Dornbush, M.E., 2014. The myriad surprises of unwanted guests: invasive plants and dynamic soil carbon pools. New Phytologist 203, 1–3.
Eisenlord, S.D., Freedman, Z., Zak, D.R., Xue, K., He, Z.L., Zhou, J.Z., 2013. Microbial mechanisms mediating increased soil C storage under elevated atmospheric N deposition. Applied and Environmental Microbiology 79, 1191–1199.
Fanin, N., Kardol, P., Farrell, M., Nilsson, M.C., Gundale, M.J., Wardle, D.A., 2019. The ratio of Gram-positive to Gram-negative bacterial PLFA markers as an indicator of carbon availability in organic soils. Soil Biology and Biochemistry 128, 111–114.
Feng, X.J., Simpson, A.J., Schlesinger, W.H., Simpson, M.J., 2010. Altered microbial community structure and organic matter composition under elevated CO_2 and N fertilization in the duke forest. Global Change Biology 16, 2104–2116.
Fornara, D.A., Tilman, D., 2012. Soil carbon sequestration in prairie grasslands increased by chronic nitrogen addition. Ecology 93 (9), 2030–2036.
Frey, S.D., Ollinger, S., Nadelhoffer, K., Bowden, R., Brzostek, E., Burton, A., Caldwell, B. A., Crow, S., Goodale, C.L., Grandy, A.S., Finzi, A.C., Kramer, M.G., Lajtha, K., LeMoine, J., Martin, M., McDowell, W.H., Minocha, R., Sadowsky, J.J., Templer, P. H., Wickings, K., 2014. Chronic nitrogen additions suppress decomposition and sequester soil carbon in temperate forests. Biogeochemistry 121, 305–316.
Funk, J.L., Vitousek, P.M., 2007. Resource-use efficiency and plant invasion in low-resource systems. Nature 446, 1079–1081.
Galloway, J.N., Townsend, A.R., Erisman, J.W., Bekunda, M., Cai, Z., Freney, J.R., Martinelli, L.A., Seitzinger, S.P., Sutton, M.A., 2008. Transformation of the nitrogen cycle: Recent trends, questions, and potential solutions. Science 320, 889.
Glenn, E.P., Nelson, S.G., Ambrose, B., Martinez, R., Soliz, D., Pabendinskas, V., Hultine, K., 2012. Comparison of salinity tolerance of three *Atriplex* spp. in well-watered and drying soils. Environmental and Experimental Botany 83, 62–72.
Griepentrog, M., Bode, S., Boeckx, P., Hagedorn, F., Heim, A., Schmidt, M.W.I., 2014. Nitrogen deposition promotes the production of new fungal residues but retards the decomposition of old residues in forest soil fractions. Global Change Biology 20, 327–340.
Hughes, R.F., Archer, S.R., Asner, G.P., Wessman, C.A., McMurtry, C., Nelson, J.I.M., Ansley, R.J., 2006. Changes in aboveground primary production and carbon and nitrogen pools accompanying woody plant encroachment in a temperate savanna. Global Change Biology 12, 1733–1747.
Jackson, R.B., Banner, J.L., Jobbagy, E.G., Pockman, W.T., Wall, D.H., 2002. Ecosystem carbon loss with woody plant invasion of grasslands. Nature 418, 623–626.
Jatana, B.S., Kitchens, C., Ray, C., Tharayil, N., 2020. Regulating the nutrient release rates from proteinaceous agricultural byproducts using organic amendments and its effect on soil chemical and microbiological properties. Biology and Fertility of Soils 1–12.
Joergensen, R.G., 2018. Amino sugars as specific indices for fungal and bacterial residues in soil. Biology and Fertility of Soils 54, 559–568.
LeBauer, D.S., Treseder, K.K., 2008. Nitrogen limitation of net primary productivity in terrestrial ecosystems is globally distributed. Ecology 89, 371–379.
Lehmann, J., Kleber, M., 2015. The contentious nature of soil organic matter. Nature 528, 60–68.
Lehmann, J., Solomon, D., Kinyangi, J., Dathe, L., Wirick, S., Jacobsen, C., 2008. Spatial complexity of soil organic matter forms at nanometre scales. Nature Geoscience 1, 238–242.
Li, Y.C., Li, Y.F., Chang, S.X., Xu, Q.F., Guo, Z.Y., Gao, Q., Qin, Z.Y., Yang, Y.F., Chen, J. H., Liang, X., 2017. Bamboo invasion of broadleaf forests altered soil fungal community closely linked to changes in soil organic C chemical composition and mineral N production. Plant and Soil 418, 507–521.
Liang, C., Balser, T.C., 2012. Warming and nitrogen deposition lessen microbial residue contribution to soil carbon pool. Nature Communications 3.
Liang, C., Duncan, D.S., Balser, T.C., Tiedje, J.M., Jackson, R.D., 2013. Soil microbial residue storage linked to soil legacy under biofuel cropping systems in southern Wisconsin, USA. Soil Biology and Biochemistry 57, 939–942.
Liang, C., Schimel, J.P., Jastrow, J.D., 2017. The importance of anabolism in microbial control over soil carbon storage. Nature Microbiology 2.
Liang, C., Amelung, W., Lehmann, J., Kastner, M., 2019. Quantitative assessment of microbial necromass contribution to soil organic matter. Global Change Biology 25, 3578–3590.
Liao, C.Z., Peng, R.H., Luo, Y.Q., Zhou, X.H., Wu, X.W., Fang, C.M., Chen, J.K., Li, B., 2008. Altered ecosystem carbon and nitrogen cycles by plant invasion: a meta-analysis. New Phytologist 177, 706–714.
Lichter, J., Billings, S.A., Ziegler, S.E., Gaindh, D., Ryals, R., Finzi, A.C., Jackson, R.B., Stemmler, E.A., Schlesinger, W.H., 2008. Soil carbon sequestration in a pine forest after 9 years of atmospheric CO_2 enrichment. Global Change Biology 14, 2910–2922.
Liu, J., Wu, N.N., Wang, H., Sun, J.F., Peng, B., Jiang, P., Bai, E., 2016. Nitrogen addition affects chemical compositions of plant tissues, litter and soil organic matter. Ecology 97, 1796–1806.
Lowe, S., Browne, M., Boudjelas, S., Poorter, M.D., 2000. 100 of the World's Worst Invasive Alien Species A Selection from the Global Invasive Species Database. The Invasive Species Specialist Group (ISSG) a Specialist Group of the Species Survival Commission. SSC) of the World Conservation Union (IUCN), p. 12.
Ma, T., Zhu, S.S., Wang, Z.H., Chen, D.M., Dai, G.H., Feng, B.W., Su, X.Y., Hu, H.F., Li, K. H., Han, W.X., Liang, C., Bai, Y.F., Feng, X.J., 2018. Divergent accumulation of microbial necromass and plant lignin components in grassland soils. Nature Communications 9.
Manzoni, S., Taylor, P., Richter, A., Porporato, A., Agren, G.I., 2012. Environmental and stoichiometric controls on microbial carbon-use efficiency in soils. New Phytologist 196, 79–91.
McTee, M.R., Lekberg, Y., Mummey, D., Rummel, A., Ramsey, P.W., 2017. Do invasive plants structure microbial communities to accelerate decomposition in intermountain grasslands? Ecology and Evolution 7, 11227–11235.
Minerovic, A.J., Valverde-Barrantes, O.J., Blackwood, C.B., 2018. Physical and microbial mechanisms of decomposition vary in importance among root orders and tree species with differing chemical and morphological traits. Soil Biology and Biochemistry 124, 142–149.
Mutabaruka, R., Hairiah, K., Cadisch, G., 2007. Microbial degradation of hydrolysable and condensed tannin polyphenol-protein complexes in soils from different land-use histories. Soil Biology and Biochemistry 39, 1479–1492.
Oksanen, J., Blanchet, F.G., Kindt, R., Legendre, P., Minchin, P., O'hara, R., Simpson, G., Solymos, P., Stevens, M., Wagner, H., 2013. Community Ecology Package. R Package Version, 2.0-2.
Olofsson, M.A., Bylund, D., 2016. Liquid chromatography with electrospray ionization and tandem mass spectrometry applied in the quantitative analysis of chitin-derived glucosamine for a Rapid estimation of fungal biomass in soil. International Journal of Analytical Chemistry 2016 (6), 1–8.
Oren, R., Ellsworth, D.S., Johnsen, K.H., Phillips, N., Ewers, B.E., Maier, C., Schafer, K.V. R., McCarthy, H., Hendrey, G., McNulty, S.G., Katul, G.G., 2001. Soil fertility limits carbon sequestration by forest ecosystems in a CO_2-enriched atmosphere. Nature 411, 469–472.
Otto, A., Simpson, M.J., 2007. Analysis of soil organic matter biomarkers by sequential chemical degradation and gas chromatography - mass spectrometry. Journal of Separation Science 30, 272–282.
Pregitzer, K.S., Burton, A.J., Zak, D.R., Talhelm, A.F., 2008. Simulated chronic nitrogen deposition increases carbon storage in Northern Temperate forests. Global Change Biology 14, 142–153.
Quideau, S.A., McIntosh, A.C.S., Norris, C.E., Lloret, E., Swallow, M.J.B., Hannam, K., 2016. Extraction and analysis of microbial phospholipid fatty acids in soils. Jove-Journal of Visualized Experiments 114.
Schindlbacher, A., Rodler, A., Kuffner, M., Kitzler, B., Sessitsch, A., Zechmeister-Boltenstern, S., 2011. Experimental warming effects on the microbial community of a temperate mountain forest soil. Soil Biology and Biochemistry 43, 1417–1425.
Schmidt, M.W., Torn, M.S., Abiven, S., Dittmar, T., Guggenberger, G., Janssens, I.A., Kleber, M., Kögel-Knabner, I., Lehmann, J., Manning, D.A., 2011. Persistence of soil organic matter as an ecosystem property. Nature 478, 49.
Shang, Z.H., 2013. Grasslandification has significant impacts on soil carbon, nitrogen and phosphorus of alpine wetlands on the Tibetan Plateau. Ecological Engineering 58, 170–179, 2013 v.2058.
Shinohara, T., Leskovar, D.I., 2014. Effects of ABA, antitranspirants, heat and drought stress on plant growth, physiology and water status of artichoke transplants. Scientia Horticulturae 165, 225–234.
Simberloff, D., Martin, J.-L., Genovesi, P., Maris, V., Wardle, D.A., Aronson, J., Courchamp, F., Galil, B., García-Berthou, E., Pascal, M., Pyšek, P., Sousa, R., Tabacchi, E., Vilà, M., 2013. Impacts of biological invasions: what's what and the way forward. Trends in Ecology & Evolution 28, 58–66.
Sokol, N.W., Bradford, M.A., 2019. Microbial formation of stable soil carbon is more efficient from belowground than aboveground input. Nature Geoscience 12, 46–53.
Stefanowicz, A.M., Stanek, M., Nobis, M., Zubek, S., 2017. Few effects of invasive plants Reynoutria japonica, Rudbeckia laciniata and Solidago gigantea on soil physical and chemical properties. The Science of the Total Environment 574, 938–946.
Stefanowicz, A.M., Majewska, M.L., Stanek, M., Nobis, M., Zubek, S., 2018. Differential influence of four invasive plant species on soil physicochemical properties in a pot experiment. Journal of Soils and Sediments 18, 1409–1423.
Strickland, M.S., Rousk, J., 2010. Considering fungal:bacterial dominance in soils - methods, controls, and ecosystem implications. Soil Biology and Biochemistry 42, 1385–1395.
Strickland, M.S., Devore, J.L., Maerz, J.C., Bradford, M.A., 2010. Grass invasion of a hardwood forest is associated with declines in belowground carbon pools. Global Change Biology 16, 1338–1350.

Suseela, V., Alpert, P., Nakatsu, C.H., Armstrong, A., Tharayil, N., 2016. Plant-soil interactions regulate the identity of soil carbon in invaded ecosystems: implication for legacy effects. Functional Ecology 30, 1227–1238.
Tamura, M., Tharayil, N., 2014. Plant litter chemistry and microbial priming regulate the accrual, composition and stability of soil carbon in invaded ecosystems. New Phytologist 203, 110–124.
Tamura, M., Suseela, V., Simpson, M., Powell, B., Tharayil, N., 2017. Plant litter chemistry alters the content and composition of organic carbon associated with soil mineral and aggregate fractions in invaded ecosystems. Global Change Biology 23, 4002–4018.
Tautges, N.E., Chiartas, J.L., Gaudin, A.C.M., O'Geen, A.T., Herrera, I., Scow, K.M., 2019. Deep soil inventories reveal that impacts of cover crops and compost on soil carbon sequestration differ in surface and subsurface soils. Global Change Biology 25, 3753–3766.
Tharayil, N., Suseela, V., Triebwasser, D.J., Preston, C.M., Gerard, P.D., Dukes, J.S., 2011. Changes in the structural composition and reactivity of Acer rubrum leaf litter tannins exposed to warming and altered precipitation: climatic stress-induced tannins are more reactive. New Phytologist 191, 132–145.
Tharayil, N., Alpert, P., Bhowmik, P., Gerard, P., 2013. Phenolic inputs by invasive species could impart seasonal variations in nitrogen pools in the introduced soils: a case study with Polygonum cuspidatum. Soil Biology and Biochemistry 57, 858–867.
Thevenot, M., Dignac, M.F., Rumpel, C., 2010. Fate of lignins in soils: a review. Soil Biology and Biochemistry 42, 1200–1211.
Treseder, K.K., 2008. Nitrogen additions and microbial biomass: a meta-analysis of ecosystem studies. Ecology Letters 11, 1111–1120.
van Kleunen, M., Weber, E., Fischer, M., 2010. A meta-analysis of trait differences between invasive and non-invasive plant species. Ecology Letters 13, 235–245.
Vestergard, M., Reinsch, S., Bengtson, P., Ambus, P., Christensen, S., 2016. Enhanced priming of old, not new soil carbon at elevated atmospheric CO_2. Soil Biology and Biochemistry 100, 140–148.
Vila, M., Espinar, J.L., Hejda, M., Hulme, P.E., Jarosik, V., Maron, J.L., Pergl, J., Schaffner, U., Sun, Y., Pysek, P., 2011. Ecological impacts of invasive alien plants: a meta-analysis of their effects on species, communities and ecosystems. Ecology Letters 14, 702–708.
Vitousek, P.M., Aber, J.D., Howarth, R.W., Likens, G.E., Matson, P.A., Schindler, D.W., Schlesinger, W.H., Tilman, D., 1997. Human alteration of the global nitrogen cycle: Sources and consequences. Ecological Applications 7, 737–750.
Waldrop, M.P., Zak, D.R., Sinsabaugh, R.L., Gallo, M., Lauber, C., 2004. Nitrogen deposition modifies soil carbon storage through changes in microbial enzymatic activity. Ecological Applications 14, 1172–1177.
Wang, J.J., Tharayil, N., Chow, A.T., Suseela, V., Zeng, H., 2015. Phenolic profile within the fine-root branching orders of an evergreen species highlights a disconnect in root tissue quality predicted by elemental- and molecular-level carbon composition. New Phytologist 206 (4), 1261–1273.
Weand, M.P., Arthur, M.A., Lovett, G.M., McCulley, R.L., Weathers, K.C., 2010. Effects of tree species and N additions on forest floor microbial communities and extracellular enzyme activities. Soil Biology and Biochemistry 42, 2161–2173.
Wei, D., Yang, Q., Zhang, J.Z., Wang, S., Chen, X.L., Zhang, X.L., Li, W.Q., 2008. Bacterial community structure and diversity in a black soil as affected by long-term fertilization. Pedosphere 18, 582–592.
Yang, W., An, S., Zhao, H., Xu, L., Qiao, Y., Cheng, X., 2016. Impacts of Spartina alterniflora invasion on soil organic carbon and nitrogen pools sizes, stability, and turnover in a coastal salt marsh of eastern China. Ecological Engineering 86, 174–182.
Yuan, Z.Y., Chen, H.Y., 2012. A global analysis of fine root production as affected by soil nitrogen and phosphorus. Proceedings of the Royal Society B: Biological Sciences 279 (1743), 3796–3802.
Zak, D.R., Holmes, W.E., Burton, A.J., Pregitzer, K.S., Talhelm, A.F., 2008. Simulated atmospheric No3- deposition increases soil organic matter by slowing decomposition. Ecological Applications 18, 2016–2027.
Zak, D.R., Argiroff, W.A., Freedman, Z.B., Upchurch, R.A., Entwistle, E.M., Romanowicz, K.J., 2019. Anthropogenic N deposition, fungal gene expression, and an increasing soil carbon sink in the Northern Hemisphere. Ecology 100.
Zhang, Z., Bhowmik, P.C., Suseela, V., 2020. Effect of soil carbon amendments in reversing the legacy effect of plant invasion. Journal of Applied Ecology 58 (1), 181–191.
Zhou, G., Xu, S., Ciais, P., Manzoni, S., Fang, J., Yu, G., Tang, X., Zhou, P., Wang, W., Yan, J., Wang, G., 2019. Climate and litter C/N ratio constrain soil organic carbon accumulation. National Science Review 6 (4), 746–757.
Ziegler, S.E., Billings, S.A., 2011. Soil nitrogen status as a regulator of carbon substrate flows through microbial communities with elevated CO_2. Journal of Geophysical Research-Biogeosciences 116.
Ziter, C., MacDougall, A.S., 2013. Nutrients and defoliation increase soil carbon inputs in grassland. Ecology 94 (1), 106–116.